Pergamon

Cement and Concrete Research 33 (2003) 763–768

CEMENT AND CONCRETE RESEARCH

Effect of particle size distribution of fly ash–cement system on the fluidity of cement pastes

Seung Heun Lee[a,*], Hong Joo Kim[a], Etsuo Sakai[b], Masaki Daimon[b]

[a]Faculty of Materials and Chemical Engineering, College of Engineering, Kunsan National University, San 68 Miryong-dong, Kunsan 573-701, South Korea
[b]Department of Metallurgy and Ceramic Science, Graduate School, Tokyo Institute of Technology, 2-12-1 O-okayama, Meguro-ku, Tokyo 152, Japan

Received 8 May 2002; accepted 4 November 2002

Abstract

This paper investigates the effect of particle size distribution of fly ash–cement system on the fluidity of the cement pastes using class F fly ash collected from the hopper attached to an electrostatic precipitator when the burning conditions and types of coal are changed at a coal-fired power plant. The unburned carbon content of fly ashes used in the experiment is less than 1.5%. To prevent the unburned carbon in fly ashes from affecting the fluidity of the pastes, polycarboxylic acid plasticizer with more saturation amount is added into the pastes for experimentation. The particle size distribution of fly ash–cement system is analyzed using *n* value of Rosin–Rammler function and the *n* value is derived with a nonlinear least squares fitting method. As the result, it is shown that the fluidity increases as the particle size distribution becomes wider, i.e., as *n* value gets smaller.

Keywords: Fly ash; Electrostatic precipitator; Fluidity; Rosin–Rammler function; *n* value

1. Introduction

Fly ash is a by-product that is collected from an electrostatic precipitator after combustion at a pulverized coal-firing boiler of a power plant. Thus, there is an increasing demand for research of fly ash from the points of environmental pollution prevention and by-product recycling. In coal-fired power plant, fly ash that passes through the combustion boiler is negatively charged by corona discharge in electrostatic precipitator. Then, it is collected at collecting electrodes and dropped onto a hopper by the operation of rappers. The electrostatic precipitator has several collection hoppers in the direction where gas moves. In most of coal-fired power plants, fly ash collected by the hopper of electrostatic precipitator is sent to a silo in a line to be stored or buried. The stored fly ash is classified by a separator according to the specification, and thus, to be used as a concrete mineral admixture and the raw material of cement. However, the fly ash collected by each hopper of electrostatic precipitator has different properties. For example, specific surface area of the fly ash increases as the collection hopper gets distance from the boiler [1–3].

The fluidity improvement of pastes by addition of fly ash has been reported mostly as follows [4–9]. (i) The density of fly ash is smaller than that of cement. Accordingly, if some of cement is replaced with fly ash by mass ratio, the paste volume of the mixture increases. (ii) Fly ash prevents cement particle from forming into blocks. (iii) Fly ash delays the hydration of cement. (iv) As fly ash is of spherical shape, it has a ball-bearing effect.

However, if fly ash with different particle size distributions is added to cement, the particle size distribution of fly ash–cement system is changed, affecting the packing density of the pastes so that the retention water of the pastes varies. Thus, it is expected that the fluidity of pastes will change [10–12].

This paper investigates the effect of particle size distribution of fly ash–cement system on the fluidity of cement pastes. The Rosin–Rammler distribution function has been used for analyzing the particle size distribution [13–16]. To prevent the influence of unburned carbon on the cement pastes, fly ashes containing less than 1.5% of unburned carbon produced at a same coal-fired power plant are used.

* Corresponding author. Tel.: +82-63-469-4733; fax: +82-63-469-4892.

E-mail address: shlee@kunsan.ac.kr (S.H. Lee).

0008-8846/02/$ – see front matter
doi:10.1016/S0008-8846(02)01054-2

In the experiment, more saturation amount of superplasticizer is added to the pastes.

2. Materials and methods

2.1. Materials

Fly ashes used in the experiment were from a coal-fired power plant in Japan. They are class F fly ashes that were collected from a hopper attached to an electrostatic precipitator after changing the burning conditions and types of bituminous coal. The A series is the fly ash generated when the load of the boiler was 600 MW while the A′ series is the fly ash when the load of the boiler was 300 MW (at night) using the same type of coal used for A series. The B series is the fly ash collected when different bituminous coal was used at the same load (600 MW) as the A series. As shown in Fig. 1, the electrostatic precipitator has a few hoppers in the direction of flue gas exhaustion. Fly ashes collected from the hoppers closest to the inlet were named A-1, A′-1, and B-1. Fly ashes collected from the second hoppers were named A-2, A′-2, and B-2. Finally, fly ashes collected from the hoppers located at the outlet were named A-3, A′-3, and B-3. The ordinary Portland cement (Blaine specific surface area, 356 m^2/kg; specific gravity, 3.15) and polycarboxylic acid superplasticizer were used to prepare paste samples for measurement of apparent viscosity.

2.2. Measurement of physical and chemical properties of fly ashes

The chemical properties of fly ashes such as chemical composition, unburned carbon content (Horiuti, Chromatic C) and loss on ignition were measured. Blaine specific surface area, specific gravity, and particle size distribution were measured to characterize the physical properties of fly ashes. A laser diffraction-type particle size analyzer (Microtrak-9320HRA) was used to measure particle size distribution and mean particle size. The particle size distribution of fly ash–cement system containing 20 vol.% of fly ash was computed from the measurement of each particle size distribution. The particle size distribution of fly ash–cement system was evaluated by using n value of Rosin–Rammler distribution function. The software Origin (version 6.1, OriginLab) was used in order to determine n value.

2.3. Measurement of apparent viscosity

Fly ashes mixed with ordinary Portland cement in 20 vol.% and the used amount of polycarboxylic acid superplasticizer was 1.6%. The sample was mixed with water at water/solid volume ratio of 0.9 for 3 min. The apparent viscosity of pastes with fly ashes was measured at 200 Pa after shear stress was changed up and down between 0 and 200 Pa at 20 °C using a rotary viscometer (Codix, Germany). The inverse of the apparent viscosity was used as the fluidity value.

3. Results and discussion

3.1. Properties of classified fly ashes by using of electrostatic precipitator

Table 1 shows the physical properties of fly ashes. The Blaine value of fly ashes increased, going from the first hopper to the third hopper, regardless of the burning conditions and types of coal, to become higher than 700 m^2/kg. The Blaine value of ordinary Portland cement was 356 m^2/kg, which was slightly greater than that of fly ashes collected from the first hopper. Mean particle size of fly ashes was 22.85–28.10 μm at the first hopper but was in the

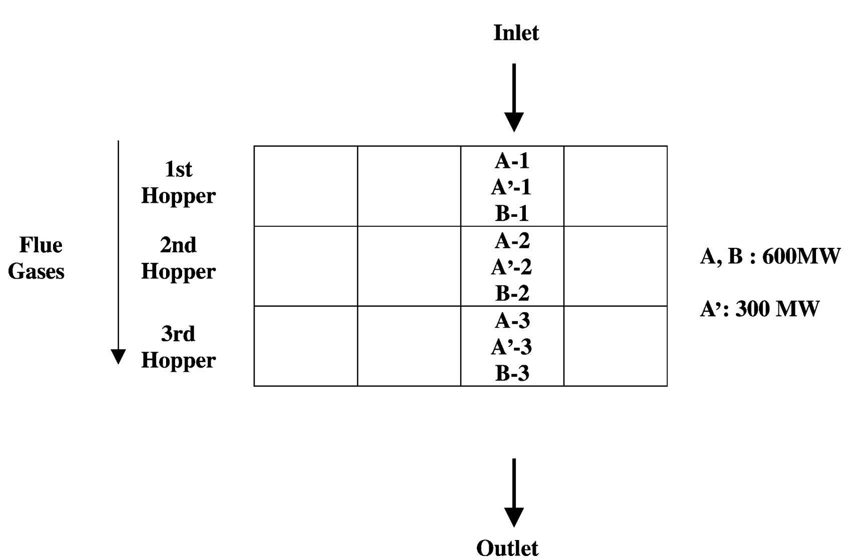

Fig. 1. The collected hoppers of the electrostatic precipitator in the coal-fired power plant.

Table 1
Physical properties of fly ashes

Fly ash	Specific gravity	Blaine value (m^2/kg)	Mean particle size (μm)
A-1	2.06	276	27.33
A-2	2.22	418	12.47
A-3	2.42	736	5.39
A′-1	2.08	358	22.85
A′-2	2.23	498	11.00
A′-3	2.40	792	5.38
B-1	2.24	264	28.10
B-2	2.33	449	12.46
B-3	2.48	729	3.74

range of 3.74–5.39 μm at the third hopper. Mean particle size of B-3 was 3.74 μm, which was slightly less than those of A-3 and A′-3. Mean particle size of ordinary Portland cement was 18.81 μm, which lay in the middle of fly ashes collected from the first and second hoppers.

Unburned carbon content and loss on ignition were in the range of 0.3–1.5% and 0.5–2.1%, respectively, which are low values in general. According to Kanazu et al. [17], who examined the flow value of mortar containing fly ashes whose unburned carbon content was in the range of 0.4–18.0%, the value tended to decrease as unburned carbon content increased but to have almost the same value in case of less than 1.5%.

Table 2 shows the chemical composition of fly ashes. The sum of SiO_2 and Al_2O_3 was higher than 85% for A and A′ series and more than 75% for B series. These represent a typical composition of class F fly ashes. Chemical composition of fly ashes according to the collection hopper showed that SiO_2 decreased from the first hopper to the third hopper. The amount of Al_2O_3, however, was slightly increased.

The sum of Fe_2O_3, alkali, and alkali earth oxides, which lowered the melting temperature of fly ashes, was about 10% for A and A′ series and about 13% for B series. There was no difference in the chemical composition due to the burning conditions. However, the chemical composition of fly ashes got affected by the type of coal. Thus, B series with a different type of bituminous coal had 7.5–8.1% of CaO, which was approximately three times greater than those of A and A′ series with more SO_3.

Table 2
Chemical analysis of fly ashes (%)

Fly ash	SiO_2	Al_2O_3	Fe_2O_3	CaO	MgO	TiO_2	Na_2O	K_2O	SO_3	C	Ignition loss
A-1	63.0	24.8	4.6	2.3	0.9	1.0	1.2	0.7	0.3	0.7	1.1
A-2	62.0	25.5	4.3	2.2	1.2	1.1	1.3	0.8	0.4	0.8	1.2
A-3	59.5	26.4	4.8	2.3	1.2	1.1	1.3	0.8	1.0	0.3	1.7
A′-1	62.1	24.9	4.2	2.0	1.1	1.1	1.2	0.8	0.5	1.5	2.1
A′-2	60.9	25.4	4.5	2.3	0.9	1.1	1.2	0.8	0.6	1.3	2.1
A′-3	59.6	26.4	4.3	2.3	1.1	1.1	1.4	0.8	1.0	0.4	1.9
B-1	61.9	18.2	5.5	7.5	2.2	0.8	1.6	0.6	0.6	1.0	1.0
B-2	58.5	20.3	5.1	8.1	2.4	0.9	1.9	0.7	0.8	1.1	1.1
B-3	55.7	22.0	5.7	7.9	2.2	1.0	2.1	0.7	1.4	0.5	0.5

3.2. Particle size distribution of fly ash–cement system

Figs. 2 and 3 show a frequency distribution and a cumulative distribution curves of fly ashes and ordinary Portland cement, respectively. Compared to the fly ashes collected from the first and second hoppers, the fly ashes collected from the third hopper showed that the range of particle size distribution got smaller while the frequency distribution indicated a normal distribution curve. Although there was some difference according to the burning conditions and types of coal, the fly ashes collected from the same hopper showed a similar pattern of particle size distribution. This is because the particle behavior inside the electrostatic precipitator heavily relies on particle diameter, meaning, the particles that passed through the combustion boiler enters the electrostatic precipitator to be collected by collecting electrode plates. Velocity (V) of particle moving at the plates is described as $V = KE^2d$, where E is the electric field strength, d is the particle diameter, and K is a constant [18]. Accordingly, the large particles are collected at the inlet of the electrostatic precipitator, i.e., the first hopper, while the small particles are collected at the third hopper, which is far from the inlet. Thus, the mean particle size becomes smaller and the range of particle size distribution gets narrower as the hopper becomes far from the boiler. Since B series derived from a different coal type has wider particle size distribution than A and A′ series, the particle size distribution of fly ashes derived from the same boiler of power plant varies according to types of coal. The particle size distribution of ordinary Portland cement shows an intermediate form of fly ashes collected from the first and second hoppers.

The Rosin–Rammler distribution function has long been used to describe the particle size distribution of powders of various types and sizes. The function is particularly suited to representing powders made by grinding, milling, and crush-

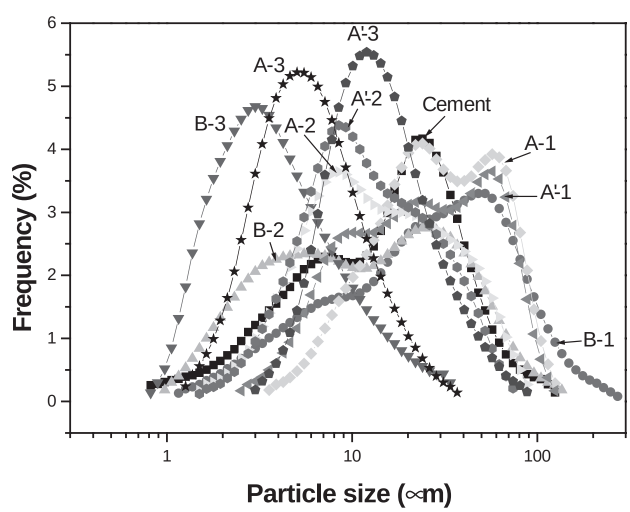

Fig. 2. Frequency particle size distribution curves for fly ashes and ordinary Portland cement.

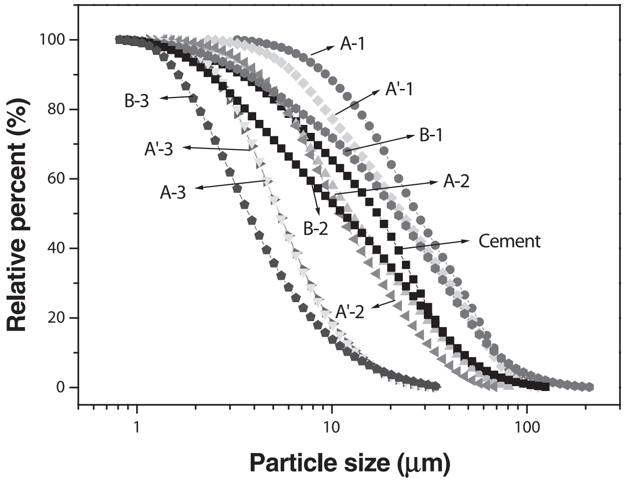

Fig. 3. Cumulative particle size distribution curves for fly ashes and ordinary Portland cement.

ing operations [13–16]. Since the powder-like cement and fly ash conform to the Rosin–Rammler distribution relatively well [15,16,19], the Rosin–Rammler distribution function is used to evaluate the particle size distribution of fly ash–cement system. Eq. (1) shows the Rosin–Rammler distribution function.

$$R(D_p) = 100\exp[-(D_p/D_e)^n] \qquad (1)$$

where $R(D_p)$ is the cumulative percentage over size (%), D_p is the corresponding particle diameter (μm), and the parameter D_e is a constant-related particle size. The exponent n is the constant indicating the width of distribution, where the smaller n, the wider the width of distribution. Taking logarithms on both sides of Eq. (1) two times,

$$\log\{\log(100/R(D_p))\} = n\log D_p - n\log D_e \qquad (2)$$

Therefore, Eq. (2) has a linear relationship on the coordinates of $\log\{\log(100/R(D_p))\}$ and $\log D_p$. However,

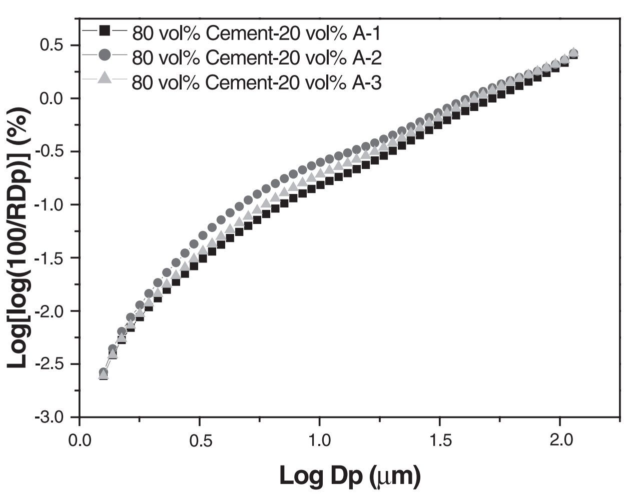

Fig. 4. Result of particle size distribution on Rosin–Rammler diagram.

as shown in Fig. 4, a good linear relationship was not derived at both ends of the line by using Eq. (2). Also, it was very difficult to find an accurate n value as it depends on the total range of particle size. To minimize errors, the experiment took nonlinear least square fitting (NLSF) in the form of Eq. (1). Here, the n and D_e values were used as parameters and a cumulative percentage oversize was selected as a dependent variable for independent variable particle size, D_p. Then, repetitive fittings were performed until chi-square (χ^2) value, the square sum of errors between theoretic value and experimental value, becomes the smallest. The results closely approached the actual values, as some of the results are shown in Fig. 5.

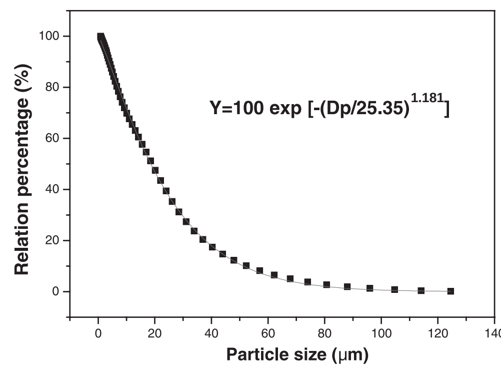

(a) 80 vol% Cement-20 vol% A-1

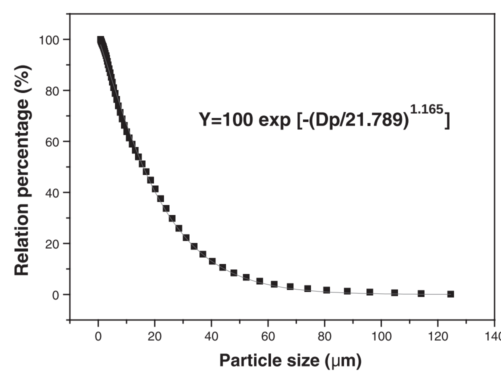

(b) 80 vol% Cement-20 vol% A-2

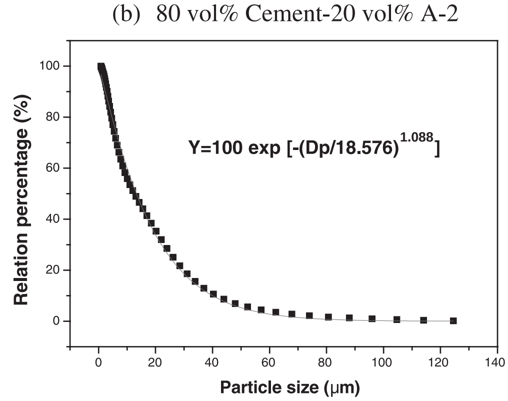

(c) 80 vol % Cement-20 vol% A-3

Fig. 5. The relationship between actual (■) and fitting (—) value for NLSF.

Table 3 shows n and D_e value of Rosin–Rammler distribution function for fly ash–cement system mixed with 20 vol.% fly ashes. In case of mixing A-1 and A-2 and A′-1 and A′-2, the n value was greater than that of ordinary Portland cement. A-3 and A′-3 showed the less value. This is because fly ashes collected from the third hopper has mean particle size of less than 6 μm with a normal distribution, as it complements the fine particles in fly ash–cement system. In case of mixing B series, regardless of the collected hopper, n value was small in comparison with other series and ordinary Portland cement. This is due to a wider range of particle size distribution.

3.3. Evaluation of fluidity of fly ash–cement pastes

Unburned carbon content of the fly ashes used in the experiment was 0.3–1.5%. Although it was very small, to prevent the unburned carbon in fly ashes from affecting the fluidity of pastes, polycarboxylic acid superplasticizer with more saturation amount was added into the cement pastes for experimentation. As for the result, adding more than 1.4% of polycarboxylic acid plasticizer made the apparent viscosity steady. Thus, 1.6% of superplasticizer was used in the experiment.

Fluidity of cement pastes mixed with 20 vol.% fly ashes is depicted in Fig. 6. Apparent viscosity is expressed with $\eta=\tau/\gamma$ (τ is the shear stress and γ is the shear rate). It corresponds to the inverse of a shear rate generated at an arbitrary shear stress (200 Pa). Thus, the inverse of apparent viscosity ($1/\tau$) is evaluated to be the fluidity. Although there is some deviation due to other factors such as the particle shape, the surface roughness and the fly ash reactivity, the fluidity of pastes tends to grow as the n value gets smaller, i.e., as the particle size distribution becomes wider. B series containing lime, a reactive material, showed a better fluidity than A and A′ series. It is thought that this is because B series had a wide particle size distribution in comparison with A and A′ series. In fact, ordinary Portland cement and fly ash particles are flocculated in concentrated suspension to form loosely associated clusters. Thus, as the packing density gets improved, the water retained inside the particle clusters becomes less so that free water relating to the fluidity increases. Thus, retention water is minimized when the small particles are ideally filled in the pores between large particles, increasing free water needed for the fluidity of cement pastes [11,12]. In case of a narrow particle size distribution, the pore between particles is bigger, thus, having more retention water. On the other hand, in case of a wide particle size distribution, small particles fill the pores, thus, increasing the packing density while decreasing the retention water, and, increasing the free water relating to the fluidity of cement pastes.

Comparison of A-2 and A′-1 with a similar n value showed that the fluidity of the paste with A-2 was 1.6 times greater than that with A′-1. Difference between A and A′ series is the burning condition of the boiler. In A series, the fly ashes were produced under the optimal burning condition while in A′ series, the fly ashes were produced at night under an unstable burning condition. Therefore, it is considered that the A′-1 had worse particle shape and surface roughness than A-2 and that the fluidity of the paste with A-2 was degraded for those reasons.

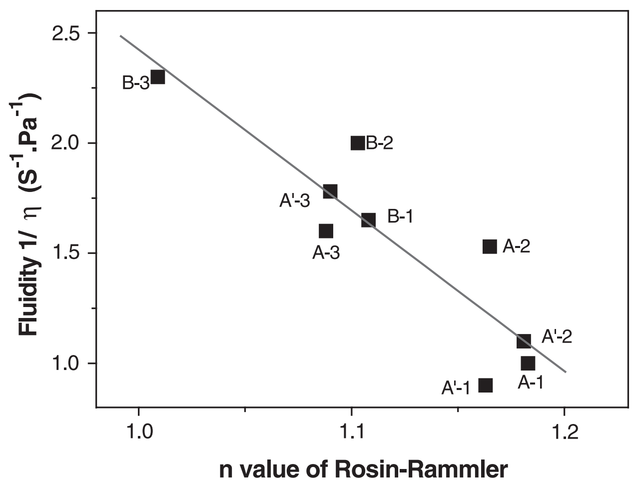

Fig. 6. The relationship between n value of Rosin–Rammler distribution function and fluidity of cement paste with fly ash.

Table 3
Rosin–Rammler parameters of fly ash–cement mixed with various fly ashes

Fly ash	n value	D_e value (μm)
Cement	1.152	22.53
A-1	1.181	25.35
A-2	1.185	21.79
A-3	1.088	18.58
A′-1	1.163	24.33
A′-2	1.183	21.12
A′-3	1.090	18.57
B-1	1.108	25.23
B-2	1.103	22.03
B-3	1.009	18.22

4. Conclusions

The main conclusions derived from this study may be summarized as follows.

1. Fly ashes collected from the rear hopper of an electrostatic precipitator of a power plant had improved fineness and particle size distribution in the form of a normal distribution curve. Also, fly ashes collected from the same site showed a similar frequency distribution although there was some difference according to the burning conditions and types of coal.
2. Rosin–Rammler model was chosen as the evaluation function for particle size distribution of fly ash–cement

system. The *n* value was found by NLSF methods. There was a tendency that the fluidity of cement pastes increased as *n* value decreased, i.e., as particle size distribution broadens. However, as there was an influence due to other factors like the particle shape and the surface roughness, there was some deviation within a small range.

Acknowledgements

The work was partly supported by the RRC program of MOST and KOSEF through the Saemankeum Environmental Research Center in Kunsan National University.

References

[1] R.T. Hemming, E.E. Berry, On the glass in coal fly ashes: recent advances, Mater. Res. Soc. Symp. Proc. 113 (1998) 3–38.
[2] S.H. Lee, E. Sakai, M. Daimon, W.K. Bang, Characterization of fly ash directly collected from electrostatic precipitator, Cem. Concr. Res. 29 (11) (1999) 1791–1797.
[3] S.H. Lee, E. Sakai, K. Watanabe, T. Yanagizawa, M. Daimon, Properties of classified fly ashes by using electrostatic precipitator and the modification of fly ashes by the removal of carbon, J. Soc. Mater. Sci. Jpn. 48 (8) (1999) 837–842.
[4] J. Paya, J. Monzo, M.V. Bornachero, E. Peris-Mora, E. Gonzalez-Lopez, Mechanical treatment of fly ashes: Part II. Particle morphologies in ground fly ash (FGA)–cement mortars, Cem. Concr. Res. 26 (2) (1966) 225–235.
[5] D. Shindo, M. Matsuoka, The effect of materials quality on properties of super workable concrete, Proc. JCI 14 (1) (1992) 78–83.
[6] N. Miura, R. Chikamatu, S. Sogo, A study on quality evaluation on high performance of concrete works, Proc. JCI Symp. Super Flowable Concr. 36 (1993) 9–16.
[7] C.S. Poon, L. Lam, Y.L. Wong, Effects of fly ash and silica fume on interfacial porosity of concrete, J. Mater. Civ. Eng. 11 (1999) 197–225.
[8] W. Jiang, D.M. Roy, Rheology in hydration and setting, in: J.M. Clarke (Ed.), Hydration and Setting in Cements, E & FN Spon Press, London, 1992, pp. 145–152.
[9] Z. Chengzhi, W. Aigin, T. Minguish, L. Xiaoyu, The filling role of pozzolanic material, Cem. Concr. Res. 26 (6) (1966) 934–947.
[10] S. Nagataki, E. Sakai, T. Takeuchi, The fluidity of fly ash–cement paste with superplasticizer, Cem. Concr. Res. 14 (5) (1984) 631–638.
[11] S. Hosino, Y. Ohba, E. Sakai, M. Daimon, The fluidity of cement paste with various classified lime stones and prepared lime stone, 49th Annual Meeting of JCA, 1995, pp. 484–489.
[12] S. Hosino, Y. Ohba, E. Sakai, M. Daimon, Relation between the properties of inorganic powders and the fluidity of cement pastes, JCA Proc. Cem. Concr. 50 (1996) 186–191.
[13] P. Rosin, E. Rammler, Regularities in the distribution of cement particles, J. Inst. Fuel. 7 (1933) 29–33.
[14] K.M. Djamarani, I.M. Clark, Characterization of particle size based on fine and coarse fractions, Powder Technol. 93 (1997) 101–108.
[15] F.T. Olorunsogo, Particle size distribution of GGBS and blending characteristics of slag cement mortars, Cem. Concr. Res. 28 (6) (1998) 907–919.
[16] S. Grzeszczyk, G. Lipowski, Effect of content and particle size distribution of high calcium fly ash on the rheological properties of cement pastes, Cem. Concr. Res. 27 (6) (1997) 907–916.
[17] T. Kanazu, K. Ito, M. Takahasi, JIS A 6201: fly ash for use in concrete, Electr. Power Civ. Eng. 274 (1998) 50–55.
[18] D. Kumio, O. Levenspiel, Fluidization engineering, in: H. Brenner (Ed.), Series in Chemical Engineering, Reed Publishing Inc., Boston, 1991, pp. 61–75.
[19] W. Aiqin, Z. Chengzhi, Z. Ningsheng, The theoretic analysis of the particle size distribution of cement system on the property of cement, Cem. Concr. Res. 29 (10) (1999) 1721–1726.